Measurements of the Electric and Magnetic Form Factors of the Neutron for Timelike Momentum Transfer

M. Ablikim,[1] M. N. Achasov,[13,b] P. Adlarson,[73] S. Ahmed,[19] R. Aliberti,[34] A. Amoroso,[72a,72c] M. R. An,[38] Q. An,[69,56] Y. Bai,[55] O. Bakina,[35] I. Balossino,[29a] Y. Ban,[45,g] V. Batozskaya,[1,43] K. Begzsuren,[31] N. Berger,[34] M. Bertani,[28a] D. Bettoni,[29a] F. Bianchi,[72a,72c] E. Bianco,[72a,72c] J. Bloms,[66] A. Bortone,[72a,72c] I. Boyko,[35] R. A. Briere,[5] A. Brueggemann,[66] H. Cai,[74] X. Cai,[1,56] A. Calcaterra,[28a] G. F. Cao,[1,61] N. Cao,[1,61] S. A. Cetin,[60a] J. F. Chang,[1,56] T. T. Chang,[75] W. L. Chang,[1,61] G. R. Che,[42] G. Chelkov,[35,a] C. Chen,[42] Chao Chen,[53] G. Chen,[1] H. S. Chen,[1,61] M. L. Chen,[1,56,61] S. J. Chen,[41] S. M. Chen,[59] T. Chen,[1,61] X. R. Chen,[30,61] X. T. Chen,[1,61] Y. B. Chen,[1,56] Y. Q. Chen,[33] Z. J. Chen,[25,h] W. S. Cheng,[72c] S. K. Choi,[10] X. Chu,[42] G. Cibinetto,[29a] S. C. Coen,[4] F. Cossio,[72c] J. J. Cui,[48] H. L. Dai,[1,56] J. P. Dai,[77] A. Dbeyssi,[19] R. E. de Boer,[4] D. Dedovich,[35] Z. Y. Deng,[1] A. Denig,[34] I. Denysenko,[35] M. Destefanis,[72a,72c] F. De Mori,[72a,72c] B. Ding,[64,1] Y. Ding,[33] Y. Ding,[39] J. Dong,[1,56] L. Y. Dong,[1,61] M. Y. Dong,[1,56,61] X. Dong,[74] S. X. Du,[79] Z. H. Duan,[41] P. Egorov,[35,a] Y. L. Fan,[74] J. Fang,[1,56] S. S. Fang,[1,61] W. X. Fang,[1] Y. Fang,[1] R. Farinelli,[29a] L. Fava,[72b,72c] F. Feldbauer,[4] G. Felici,[28a] C. Q. Feng,[69,56] J. H. Feng,[57] K Fischer,[67] M. Fritsch,[4] C. Fritzsch,[66] C. D. Fu,[1] Y. W. Fu,[1] H. Gao,[61] Y. N. Gao,[45,g] Yang Gao,[69,56] S. Garbolino,[72c] I. Garzia,[29a,29b] P. T. Ge,[74] Z. W. Ge,[41] C. Geng,[57] E. M. Gersabeck,[65] A Gilman,[67] K. Goetzen,[14] L. Gong,[39] W. X. Gong,[1,56] W. Gradl,[34] S. Gramigna,[29a,29b] M. Greco,[72a,72c] M. H. Gu,[1,56] Y. T. Gu,[16] C. Y Guan,[1,61] Z. L. Guan,[22] A. Q. Guo,[30,61] L. B. Guo,[40] R. P. Guo,[47] Y. P. Guo,[12,f] A. Guskov,[35,a] X. T. H.,[1,61] W. Y. Han,[38] X. Q. Hao,[20] F. A. Harris,[63] K. K. He,[53] K. L. He,[1,61] F. H. Heinsius,[4] C. H. Heinz,[34] Y. K. Heng,[1,56,61] C. Herold,[58] T. Holtmann,[4] P. C. Hong,[12,f] G. Y. Hou,[1,61] Y. R. Hou,[61] Z. L. Hou,[1] H. M. Hu,[1,61] J. F. Hu,[54,i] T. Hu,[1,56,61] Y. Hu,[1] G. S. Huang,[69,56] K. X. Huang,[57] L. Q. Huang,[30,61] X. T. Huang,[48] Y. P. Huang,[1] T. Hussain,[71] N Hüsken,[27,34] W. Imoehl,[27] M. Irshad,[69,56] J. Jackson,[27] S. Jaeger,[4] S. Janchiv,[31] J. H. Jeong,[10] Q. Ji,[1] Q. P. Ji,[20] X. B. Ji,[1,61] X. L. Ji,[1,56] Y. Y. Ji,[48] Z. K. Jia,[69,56] P. C. Jiang,[45,g] S. S. Jiang,[38] T. J. Jiang,[17] X. S. Jiang,[1,56,61] Y. Jiang,[61] J. B. Jiao,[48] Z. Jiao,[23] S. Jin,[41] Y. Jin,[64] M. Q. Jing,[1,61] T. Johansson,[73] X. K.,[1] S. Kabana,[32] N. Kalantar-Nayestanaki,[62] X. L. Kang,[9] X. S. Kang,[39] R. Kappert,[62] M. Kavatsyuk,[62] B. C. Ke,[79] A. Khoukaz,[66] R. Kiuchi,[1] R. Kliemt,[14] L. Koch,[36] O. B. Kolcu,[60a] B. Kopf,[4] M. Kuessner,[4] A. Kupsc,[43,73] W. Kühn,[36] J. J. Lane,[65] J. S. Lange,[36] P. Larin,[19] A. Lavania,[26] L. Lavezzi,[72a,72c] T. T. Lei,[69,k] Z. H. Lei,[69,56] H. Leithoff,[34] M. Lellmann,[34] T. Lenz,[34] C. Li,[46] C. Li,[42] C. H. Li,[38] Cheng Li,[69,56] D. M. Li,[79] F. Li,[1,56] G. Li,[1] H. Li,[69,56] H. B. Li,[1,61] H. J. Li,[20] H. N. Li,[54,i] Hui Li,[42] J. R. Li,[59] J. S. Li,[57] J. W. Li,[48] Ke Li,[1] L. J Li,[1,61] L. K. Li,[1] Lei Li,[3] M. H. Li,[42] P. R. Li,[37,j,k] S. X. Li,[12] T. Li,[48] W. D. Li,[1,61] W. G. Li,[1] X. H. Li,[69,56] X. L. Li,[48] Xiaoyu Li,[1,61] Y. G. Li,[45,g] Z. J. Li,[57] Z. X. Li,[16] Z. Y. Li,[57] C. Liang,[41] H. Liang,[33] H. Liang,[1,61] H. Liang,[69,56] Y. F. Liang,[52] Y. T. Liang,[30,61] G. R. Liao,[15] L. Z. Liao,[48] J. Libby,[26] A. Limphirat,[58] D. X. Lin,[30,61] T. Lin,[1] B. X. Liu,[74] B. J. Liu,[1] C. Liu,[33] C. X. Liu,[1] D. Liu,[19,69] F. H. Liu,[51] Fang Liu,[1] Feng Liu,[6] G. M. Liu,[54,i] H. Liu,[37,j,k] H. B. Liu,[16] H. M. Liu,[1,61] Huanhuan Liu,[1] Huihui Liu,[21] J. B. Liu,[69,56] J. L. Liu,[70] J. Y. Liu,[1,61] K. Liu,[1] K. Y. Liu,[39] Ke Liu,[22] L. Liu,[69,56] L. C. Liu,[42] Lu Liu,[42] M. H. Liu,[12,f] P. L. Liu,[1] Q. Liu,[61] S. B. Liu,[69,56] T. Liu,[12,f] W. K. Liu,[42] W. M. Liu,[69,56] X. Liu,[37,j,k] Y. Liu,[37,j,k] Y. B. Liu,[42] Z. A. Liu,[1,56,61] Z. Q. Liu,[48] X. C. Lou,[1,56,61] F. X. Lu,[57] H. J. Lu,[23] J. G. Lu,[1,56] X. L. Lu,[1] Y. Lu,[7] Y. P. Lu,[1,56] Z. H. Lu,[1,61] C. L. Luo,[40] M. X. Luo,[78] T. Luo,[12,f] X. L. Luo,[1,56] X. R. Lyu,[61] Y. F. Lyu,[42] F. C. Ma,[39] H. L. Ma,[1] J. L. Ma,[1,61] L. L. Ma,[48] M. M. Ma,[1,61] Q. M. Ma,[1] R. Q. Ma,[1,61] R. T. Ma,[61] X. Y. Ma,[1,56] Y. Ma,[45,g] F. E. Maas,[19] M. Maggiora,[72a,72c] S. Maldaner,[4] S. Malde,[67] A. Mangoni,[28b] Y. J. Mao,[45,g] Z. P. Mao,[1] S. Marcello,[72a,72c] Z. X. Meng,[64] J. G. Messchendorp,[14,62] G. Mezzadri,[29a] H. Miao,[1,61] T. J. Min,[41] R. E. Mitchell,[27] X. H. Mo,[1,56,61] N. Yu. Muchnoi,[13,b] Y. Nefedov,[35] F. Nerling,[19,d] I. B. Nikolaev,[13,b] Z. Ning,[1,56] S. Nisar,[11,l] Y. Niu,[48] S. L. Olsen,[61] Q. Ouyang,[1,56,61] S. Pacetti,[28b,28c] X. Pan,[53] Y. Pan,[55] A. Pathak,[33] Y. P. Pei,[69,56] M. Pelizaeus,[4] H. P. Peng,[69,56] K. Peters,[14,d] J. L. Ping,[40] R. G. Ping,[1,61] S. Plura,[34] S. Pogodin,[35] V. Prasad,[32] F. Z. Qi,[1] H. Qi,[69,56] H. R. Qi,[59] M. Qi,[41] T. Y. Qi,[12,f] S. Qian,[1,56] W. B. Qian,[61] C. F. Qiao,[61] J. J. Qin,[70] L. Q. Qin,[15] X. P. Qin,[12,f] X. S. Qin,[48] Z. H. Qin,[1,56] J. F. Qiu,[1] S. Q. Qu,[59] C. F. Redmer,[34] K. J. Ren,[38] A. Rivetti,[72c] V. Rodin,[62] M. Rolo,[72c] G. Rong,[1,61] Ch. Rosner,[19] S. N. Ruan,[42] A. Sarantsev,[35,c] Y. Schelhaas,[34] K. Schoenning,[73] M. Scodeggio,[29a,29b] K. Y. Shan,[12,f] W. Shan,[24] X. Y. Shan,[69,56] J. F. Shangguan,[53] L. G. Shao,[1,61] M. Shao,[69,56] C. P. Shen,[12,f] H. F. Shen,[1,61] W. H. Shen,[61] X. Y. Shen,[1,61] B. A. Shi,[61] H. C. Shi,[69,56] J. Y. Shi,[1] Q. Q. Shi,[53] R. S. Shi,[1,61] X. Shi,[1,56] J. J. Song,[20] T. Z. Song,[57] W. M. Song,[33,1] Y. X. Song,[45,g] S. Sosio,[72a,72c] S. Spataro,[72a,72c] F. Stieler,[34] Y. J. Su,[61] G. B. Sun,[74] G. X. Sun,[1] H. Sun,[61] H. K. Sun,[1] J. F. Sun,[20] K. Sun,[59] L. Sun,[74] S. S. Sun,[1,61] T. Sun,[1,61] W. Y. Sun,[33] Y. Sun,[9] Y. J. Sun,[69,56] Y. Z. Sun,[1] Z. T. Sun,[48] Y. X. Tan,[69,56] C. J. Tang,[52] G. Y. Tang,[1] J. Tang,[57] Y. A. Tang,[74] L. Y Tao,[70] Q. T. Tao,[25,h] M. Tat,[67]

J. X. Teng,[69,56] V. Thoren,[73] W. H. Tian,[50] W. H. Tian,[57] Y. Tian,[30,61] Z. F. Tian,[74] I. Uman,[60b] B. Wang,[1] B. L. Wang,[61] Bo Wang,[69,56] C. W. Wang,[41] D. Y. Wang,[45,g] F. Wang,[70] H. J. Wang,[37,j,k] H. P. Wang,[1,61] K. Wang,[1,56] L. L. Wang,[1] M. Wang,[48] Meng Wang,[1,61] S. Wang,[12,f] T. Wang,[12,f] T. J. Wang,[42] W. Wang,[57] W. Wang,[70] W. H. Wang,[74] W. P. Wang,[69,56] X. Wang,[45,g] X. F. Wang,[37,j,k] X. J. Wang,[38] X. L. Wang,[12,f] Y. Wang,[59] Y. D. Wang,[44] Y. F. Wang,[1,56,61] Y. H. Wang,[46] Y. N. Wang,[44] Y. Q. Wang,[1] Yaqian Wang,[18,1] Yi Wang,[59] Z. Wang,[1,56] Z. L. Wang,[70] Z. Y. Wang,[1,61] Ziyi Wang,[61] D. Wei,[68] D. H. Wei,[15] F. Weidner,[66] S. P. Wen,[1] C. W. Wenzel,[4] U. Wiedner,[4] G. Wilkinson,[67] M. Wolke,[73] L. Wollenberg,[4] C. Wu,[38] J. F. Wu,[1,61] L. H. Wu,[1] L. J. Wu,[1,61] X. Wu,[12,f] X. H. Wu,[33] Y. Wu,[69] Y. J Wu,[30] Z. Wu,[1,56] L. Xia,[69,56] X. M. Xian,[38] T. Xiang,[45,g] D. Xiao,[37,j,k] G. Y. Xiao,[41] H. Xiao,[12,f] S. Y. Xiao,[1] Y. L. Xiao,[12,f] Z. J. Xiao,[40] C. Xie,[41] X. H. Xie,[45,g] Y. Xie,[48] Y. G. Xie,[1,56] Y. H. Xie,[6] Z. P. Xie,[69,56] T. Y. Xing,[1,61] C. F. Xu,[1,61] C. J. Xu,[57] G. F. Xu,[1] H. Y. Xu,[64] Q. J. Xu,[17] W. L. Xu,[64] X. P. Xu,[53] Y. C. Xu,[76] Z. P. Xu,[41] F. Yan,[12,f] L. Yan,[12,f] W. B. Yan,[69,56] W. C. Yan,[79] X. Q Yan,[1] H. J. Yang,[49,e] H. L. Yang,[33] H. X. Yang,[1] Tao Yang,[1] Y. Yang,[12,f] Y. F. Yang,[42] Y. X. Yang,[1,61] Yifan Yang,[1,61] M. Ye,[1,56] M. H. Ye,[8] J. H. Yin,[1] Z. Y. You,[57] B. X. Yu,[1,56,61] C. X. Yu,[42] G. Yu,[1,61] T. Yu,[70] X. D. Yu,[45,g] C. Z. Yuan,[1,61] L. Yuan,[2] S. C. Yuan,[1] X. Q. Yuan,[1] Y. Yuan,[1,61] Z. Y. Yuan,[57] C. X. Yue,[38] A. A. Zafar,[71] F. R. Zeng,[48] X. Zeng,[12,f] Y. Zeng,[25,h] Y. J. Zeng,[1,61] X. Y. Zhai,[33] Y. H. Zhan,[57] A. Q. Zhang,[1,61] B. L. Zhang,[1,61] B. X. Zhang,[1] D. H. Zhang,[42] G. Y. Zhang,[20] H. Zhang,[69] H. H. Zhang,[57] H. H. Zhang,[33] H. Q. Zhang,[1,56,61] H. Y. Zhang,[1,56] J. J. Zhang,[50] J. L. Zhang,[75] J. Q. Zhang,[40] J. W. Zhang,[1,56,61] J. X. Zhang,[37,j,k] J. Y. Zhang,[1] J. Z. Zhang,[1,61] Jiawei Zhang,[1,61] L. M. Zhang,[59] L. Q. Zhang,[57] Lei Zhang,[41] P. Zhang,[1] Q. Y. Zhang,[38,79] Shuihan Zhang,[1,61] Shulei Zhang,[25,h] X. D. Zhang,[44] X. M. Zhang,[1] X. Y. Zhang,[48] X. Y. Zhang,[53] Y. Zhang,[67] Y. T. Zhang,[79] Y. H. Zhang,[1,56] Yan Zhang,[69,56] Yao Zhang,[1] Z. H. Zhang,[1] Z. L. Zhang,[33] Z. Y. Zhang,[74] Z. Y. Zhang,[42] G. Zhao,[1] J. Zhao,[38] J. Y. Zhao,[1,61] J. Z. Zhao,[1,56] Lei Zhao,[69,56] Ling Zhao,[1] M. G. Zhao,[42] S. J. Zhao,[79] Y. B. Zhao,[1,56] Y. X. Zhao,[30,61] Z. G. Zhao,[69,56] A. Zhemchugov,[35,a] B. Zheng,[70] J. P. Zheng,[1,56] W. J. Zheng,[1,61] Y. H. Zheng,[61] B. Zhong,[40] X. Zhong,[57] H. Zhou,[48] L. P. Zhou,[1,61] X. Zhou,[74] X. R. Zhou,[69,56] X. Y. Zhou,[38] Y. Z. Zhou,[12,f] J. Zhu,[42] K. Zhu,[1] K. J. Zhu,[1,56,61] L. Zhu,[33] L. X. Zhu,[61] S. H. Zhu,[68] S. Q. Zhu,[41] T. J. Zhu,[12,f] W. J. Zhu,[12,f] Y. C. Zhu,[69,56] Z. A. Zhu,[1,61] J. H. Zou,[1] and J. Zu[69,56]

(BESIII Collaboration)

[1]*Institute of High Energy Physics, Beijing 100049, People's Republic of China*
[2]*Beihang University, Beijing 100191, People's Republic of China*
[3]*Beijing Institute of Petrochemical Technology, Beijing 102617, People's Republic of China*
[4]*Bochum Ruhr-University, D-44780 Bochum, Germany*
[5]*Carnegie Mellon University, Pittsburgh, Pennsylvania 15213, USA*
[6]*Central China Normal University, Wuhan 430079, People's Republic of China*
[7]*Central South University, Changsha 410083, People's Republic of China*
[8]*China Center of Advanced Science and Technology, Beijing 100190, People's Republic of China*
[9]*China University of Geosciences, Wuhan 430074, People's Republic of China*
[10]*Chung-Ang University, Seoul 06974, Republic of Korea*
[11]*COMSATS University Islamabad, Lahore Campus, Defence Road, Off Raiwind Road, 54000 Lahore, Pakistan*
[12]*Fudan University, Shanghai 200433, People's Republic of China*
[13]*G.I. Budker Institute of Nuclear Physics SB RAS (BINP), Novosibirsk 630090, Russia*
[14]*GSI Helmholtzcentre for Heavy Ion Research GmbH, D-64291 Darmstadt, Germany*
[15]*Guangxi Normal University, Guilin 541004, People's Republic of China*
[16]*Guangxi University, Nanning 530004, People's Republic of China*
[17]*Hangzhou Normal University, Hangzhou 310036, People's Republic of China*
[18]*Hebei University, Baoding 071002, People's Republic of China*
[19]*Helmholtz Institute Mainz, Staudinger Weg 18, D-55099 Mainz, Germany*
[20]*Henan Normal University, Xinxiang 453007, People's Republic of China*
[21]*Henan University of Science and Technology, Luoyang 471003, People's Republic of China*
[22]*Henan University of Technology, Zhengzhou 450001, People's Republic of China*
[23]*Huangshan College, Huangshan 245000, People's Republic of China*
[24]*Hunan Normal University, Changsha 410081, People's Republic of China*
[25]*Hunan University, Changsha 410082, People's Republic of China*
[26]*Indian Institute of Technology Madras, Chennai 600036, India*
[27]*Indiana University, Bloomington, Indiana 47405, USA*

[28a]INFN Laboratori Nazionali di Frascati, INFN Laboratori Nazionali di Frascati, I-00044, Frascati, Italy
[28b]INFN Sezione di Perugia, I-06100, Perugia, Italy
[28c]University of Perugia, I-06100, Perugia, Italy
[29a]INFN Sezione di Ferrara, INFN Sezione di Ferrara, I-44122, Ferrara, Italy
[29b]University of Ferrara, I-44122, Ferrara, Italy
[30]Institute of Modern Physics, Lanzhou 730000, People's Republic of China
[31]Institute of Physics and Technology, Peace Avenue 54B, Ulaanbaatar 13330, Mongolia
[32]Instituto de Alta Investigación, Universidad de Tarapacá, Casilla 7D, Arica 1000000, Chile
[33]Jilin University, Changchun 130012, People's Republic of China
[34]Johannes Gutenberg University of Mainz, Johann-Joachim-Becher-Weg 45, D-55099 Mainz, Germany
[35]Joint Institute for Nuclear Research, 141980 Dubna, Moscow region, Russia
[36]Justus-Liebig-Universitaet Giessen, II. Physikalisches Institut, Heinrich-Buff-Ring 16, D-35392 Giessen, Germany
[37]Lanzhou University, Lanzhou 730000, People's Republic of China
[38]Liaoning Normal University, Dalian 116029, People's Republic of China
[39]Liaoning University, Shenyang 110036, People's Republic of China
[40]Nanjing Normal University, Nanjing 210023, People's Republic of China
[41]Nanjing University, Nanjing 210093, People's Republic of China
[42]Nankai University, Tianjin 300071, People's Republic of China
[43]National Centre for Nuclear Research, Warsaw 02-093, Poland
[44]North China Electric Power University, Beijing 102206, People's Republic of China
[45]Peking University, Beijing 100871, People's Republic of China
[46]Qufu Normal University, Qufu 273165, People's Republic of China
[47]Shandong Normal University, Jinan 250014, People's Republic of China
[48]Shandong University, Jinan 250100, People's Republic of China
[49]Shanghai Jiao Tong University, Shanghai 200240, People's Republic of China
[50]Shanxi Normal University, Linfen 041004, People's Republic of China
[51]Shanxi University, Taiyuan 030006, People's Republic of China
[52]Sichuan University, Chengdu 610064, People's Republic of China
[53]Soochow University, Suzhou 215006, People's Republic of China
[54]South China Normal University, Guangzhou 510006, People's Republic of China
[55]Southeast University, Nanjing 211100, People's Republic of China
[56]State Key Laboratory of Particle Detection and Electronics, Beijing 100049, Hefei 230026, People's Republic of China
[57]Sun Yat-Sen University, Guangzhou 510275, People's Republic of China
[58]Suranaree University of Technology, University Avenue 111, Nakhon Ratchasima 30000, Thailand
[59]Tsinghua University, Beijing 100084, People's Republic of China
[60a]Turkish Accelerator Center Particle Factory Group, Istinye University, 34010, Istanbul, Turkey
[60b]Near East University, Nicosia, North Cyprus, 99138, Mersin 10, Turkey
[61]University of Chinese Academy of Sciences, Beijing 100049, People's Republic of China
[62]University of Groningen, NL-9747 AA Groningen, Netherlands
[63]University of Hawaii, Honolulu, Hawaii 96822, USA
[64]University of Jinan, Jinan 250022, People's Republic of China
[65]University of Manchester, Oxford Road, Manchester, M13 9PL, United Kingdom
[66]University of Muenster, Wilhelm-Klemm-Strasse 9, 48149 Muenster, Germany
[67]University of Oxford, Keble Road, Oxford OX13RH, United Kingdom
[68]University of Science and Technology Liaoning, Anshan 114051, People's Republic of China
[69]University of Science and Technology of China, Hefei 230026, People's Republic of China
[70]University of South China, Hengyang 421001, People's Republic of China
[71]University of the Punjab, Lahore-54590, Pakistan
[72a]University of Turin and INFN, University of Turin, I-10125, Turin, Italy
[72b]University of Eastern Piedmont, I-15121, Alessandria, Italy
[72c]INFN, I-10125, Turin, Italy
[73]Uppsala University, Box 516, SE-75120 Uppsala, Sweden
[74]Wuhan University, Wuhan 430072, People's Republic of China
[75]Xinyang Normal University, Xinyang 464000, People's Republic of China

[76]Yantai University, Yantai 264005, People's Republic of China
[77]Yunnan University, Kunming 650500, People's Republic of China
[78]Zhejiang University, Hangzhou 310027, People's Republic of China
[79]Zhengzhou University, Zhengzhou 450001, People's Republic of China

(Received 15 December 2022; revised 27 February 2023; accepted 23 March 2023; published 14 April 2023; corrected 27 June 2023)

We present the first measurements of the electric and magnetic form factors of the neutron in the timelike (positive q^2) region as function of four-momentum transfer. We explored the differential cross sections of the reaction $e^+e^- \to \bar{n}n$ with data collected with the BESIII detector at the BEPCII accelerator, corresponding to an integrated luminosity of 354.6 pb^{-1} in total at twelve center-of-mass energies between $\sqrt{s} = 2.0$–2.95 GeV. A relative uncertainty of 18% and 12% for the electric and magnetic form factors, respectively, is achieved at $\sqrt{s} = 2.3935$ GeV. Our results are comparable in accuracy to those from electron scattering in the comparable spacelike region of four-momentum transfer. The electromagnetic form factor ratio $R_{\mathrm{em}} \equiv |G_E|/|G_M|$ is within the uncertainties close to unity. We compare our result on $|G_E|$ and $|G_M|$ to recent model predictions, and the measurements in the spacelike region to test the analyticity of electromagnetic form factors.

DOI: 10.1103/PhysRevLett.130.151905

Proton and neutron are the fundamental building blocks of atomic nuclei. Their complex internal structure emerges from quantum chromodynamics (QCD) but is not accessible from *ab initio* calculations in the nonperturbative regime of QCD governed by quark confinement [1] and gluon self-coupling [2]. On the other hand, measurements of the electromagnetic form factors (EMFFs) of the nucleon are straightforward [3]. EMFFs have long since served as a testing ground for the understanding of QCD at low momentum transfer q^2. Since Hofstadter's ground-breaking measurements [4], various experiments at different facilities successfully measured nucleon EMFFs [5] in electron scattering with increasing precision, providing important input for theoretical calculations of nucleon properties [6,7], in particular the size of the neutron charge radius [8]. A spin-$\frac{1}{2}$ particle, such as the nucleon, is described by two EMFFs, $G_E(q^2)$ and $G_M(q^2)$, which are Fourier transforms of the intrinsic electric and magnetic distributions of the nucleon in the Breit frame [9]. Depending on the sign of q^2 of the virtual exchange photon, we can distinguish two types of reactions. The spacelike (SL) region of negative q^2 can be accessed in lepton scattering, the timelike (TL) region of positive q^2 in annihilation reactions (see Fig. 1).

Precise measurements of scattering of leptons with neutrons [10–13] are far more difficult than with protons due to the absence of free neutron targets. Possible alternatives like deuterons inevitably introduce uncertainties from nuclear binding corrections. On the other hand, free protons and neutrons are directly accessible in the TL region. Measurements of the TL EMFFs of the proton have significantly gained precision over recent years [14–19]. However, data with large statistics from e^+e^- annihilation reactions has been rare. The first measurements of the neutron TL EMFFs were reported in the 1990s by the FENICE [20] and the DM2 [21] experiments and two other measurements were reported by the SND experiment [22,23]. A precise measurement of the neutron effective form factors $|G|$ was recently published by the BESIII Collaboration [24]. However, so far no separate result for G_E and G_M is available due to the difficulties in (anti-)neutron detection and efficiency calibration. These difficulties have prevented a detailed analysis of angular-dependent differential cross sections.

In this Letter, we report the first model-independent measurement of separate neutron EMFF moduli $|G_E|$ and $|G_M|$ in the TL regime by exploring the differential cross sections of the reaction $e^+e^- \to \bar{n}n$ with the data collected by the BESIII [25] experiment at the BEPCII [26] collider. Compared with the total cross sections, the differential cross sections provide more information to determine scattering amplitudes of distinguished partial waves [27] in order to

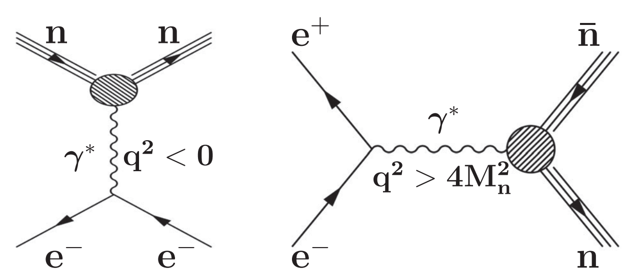

FIG. 1. The lowest order Feynman diagram for the SL process (left) $e^-n \to e^-n$ and the TL process (right) $e^+e^- \to n\bar{n}$. Here, γ^* represents the virtual photon transferring the four-momentum squared q^2 of the reaction. The gray circle represents the internal nucleon structure parameterized by the EMFFs.

verify the analyticity of EMFFs and to test various nucleon models. The data analyzed in this work corresponds to a total integrated luminosity $\mathcal{L}_{\rm int} = 354.6\ \mathrm{pb}^{-1}$ [28,29] at twelve center-of-mass energies (c.m.) between $\sqrt{s} = 2.0$ and 2.95 GeV, and is grouped into five energy intervals to extract the EMFFs. An additional dataset with 10087 ± 44 million J/ψ events [30] has been used for a precise data-driven calibration of the $n(\bar{n})$ detection efficiency with the processes $J/\psi \to \bar{p}\pi n(p\pi\bar{n})$, and an investigation of identification and reconstruction of neutral particles using the processes $J/\psi \to n\bar{n}$, $J/\psi \to \pi^+\pi^-\pi^0(\to \gamma\gamma)$, and $e^+e^- \to \gamma\gamma$.

The moduli of the electric and magnetic form factors of the neutron can be obtained by comparing the theoretical prediction to the experimentally accessible differential Born cross section as discussed in [31]

$$\frac{N^{\rm bin}}{\mathcal{L}\mathcal{E}^{\rm MC}\mathcal{E}^{\rm cor}(1+\delta)} = \int_{\rm bin} \frac{\pi\alpha^2\beta C}{2s}|G_M|^2[(1+\cos^2\theta_{\bar{n}}) + \tau R_{\rm em}^2 \sin^2\theta_{\bar{n}}]d\cos\theta_{\bar{n}},$$
$$\tau = \frac{4M_n^2}{s}. \quad (1)$$

Here, $s \equiv q^2$ represents the c.m. energy squared of the electron-positron system, M_n the neutron mass, $\beta = \sqrt{1-\tau}$ its velocity, and C the Coulomb enhancement factor accounting for the electromagnetic interaction between the outgoing baryons, which is equal to 1 for neutral baryons. Furthermore, $\cos\theta_{\bar{n}}$ is the cosine of the $\bar{n}$ polar angle along the positron beam direction in the electron-positron c.m. frame, $|G_M|$ the modulus of the magnetic form factor, and $R_{\rm em} = |G_E|/|G_M|$ the ratio of the moduli of the electric and magnetic form factors. The differential Born cross section of Eq. (1), is calculated using the luminosity $\mathcal{L}$, the signal reconstruction efficiency $\mathcal{E}^{\rm MC}$ and its correction $\mathcal{E}^{\rm cor}$, the next-to-leading-order radiation and vacuum-polarization correction $(1+\delta)$, and the signal yield $N^{\rm bin}$ per $\cos\theta_{\bar{n}}$ bin. We integrate over the bin width in accordance to histograms of angular distribution as will be discussed below.

The final state of the signal process contains one antineutron and one neutron. Hence our data analysis strategy is based on the rejection of events with charged tracks in the multilayer drift chamber (MDC). For each event, the most energetic shower in the electromagnetic calorimeter (EMC) within the polar angle range of $|\cos\theta| < 0.7$ and a deposited energy within (0.5, 2.0) GeV is considered as a $\bar{n}$ candidate. This shower is further associated with a response in the time-of-flight (TOF) system aggregating all hits within an azimuthal angle span of 6 TOF plastic scintillators along the $\bar{n}$ momentum. To avoid a potential bias and to provide a cross-check, events are classified into three categories ($i = A, B, C$) depending on the detector responses to $n\bar{n}$ particles. Events with responses from knockoff protons interaction in the TOF plastic scintillators from both particles and one associated hadronic shower registered in the EMC from the antineutron are classified as category A. Events with showers in the EMC from both particles, but only one measured knockoff proton interaction in the TOF from the anti-neutron are assigned to category B. Events lacking any TOF responses but with reconstructed hadronic showers in the EMC from both particles are classified as category C. Each event belongs to not more than one category. These categories not only provide a reliable cross-check but also guarantee a better precision using an inverse-variance weighting technique. The selection method for the three categories is described in details in Ref. [24].

With surviving events for each category aforementioned, $\cos\theta_{\bar{n}}$ of the antineutron is filled in histograms of 7 equidistant bins within $-0.7 < \cos\theta_{\bar{n}} < 0.7$. For category A, signal events are characterized by the time difference ΔT_n between the time measured with the TOF and the expected flight time calculated from the neutron's momentum and flight path, respectively. For category B and C, signal events are characterized by the opening angle $\sphericalangle_{\bar{n}}^{n}$ between neutron and antineutron as measured with the EMC. Since the surviving events still contain contributions coming mainly from the beam-related background and the $e^+e^- \to \gamma\gamma$ background, we use a composite model taking into account the background ($\mathcal{M}^b$) and signal ($\mathcal{M}^s$) distributions to fit data and determine the number of reconstructed signal events $N_i^{\rm bin}(\cos\theta_{\bar{n}})$ ($i = A, B, C$) at a given $\cos\theta_{\bar{n}}$ bin:

$$\mathcal{M}_i(x) = N_i^{\rm bin}\mathcal{M}_i^s(x) + N_i^b\mathcal{M}_i^b(x),$$
$$x = \Delta T_n \quad \text{or} \quad \sphericalangle_{\bar{n}}^{n}, \quad \forall \quad \cos\theta_{\bar{n}} \in (-0.7, 0.7). \quad (2)$$

The signal (background) distribution is modeled with the MC simulation samples of the signal (background) process generated with ConExc event generator or control samples. As an example, Fig. 2 shows the extraction of signal yield

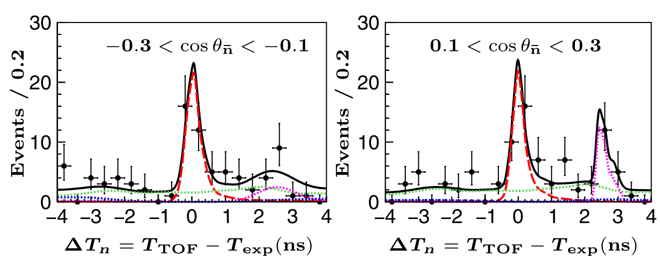

FIG. 2. Fit to the ΔT_n distribution at $\sqrt{s} = 2.1250$ GeV in (left) the third $\cos\theta_{\bar{n}}$ bin and (right) the fifth bin. Data are shown as black dots with error bars, the total fit as the black line, the signal component as the red dashed line, the $e^-e^+ \to \gamma\gamma$ background components as the magenta dashed line, and the beam-related background components as the blue dashed line. The asymmetrical uncertainties for the data are determined from the Poisson distribution to take into account the low statistics in most bins.

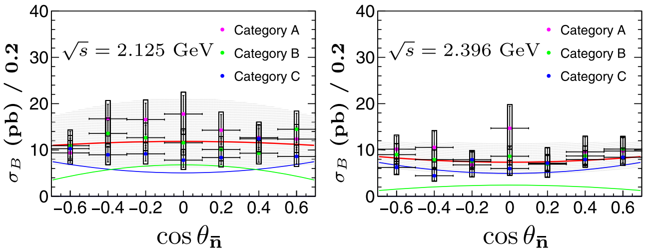

FIG. 3. A simultaneous fitting to the differential cross sections at $\sqrt{s} = 2.1250$ and 2.3964 GeV for three categories. Data are shown as colorful dots with error bars, the total fit as a red line and a gray band (68% C.L.), the $|G_M|^2$ component as the blue line, and the $\tau|G_E|^2$ component as the green line. The asymmetrical uncertainties for the data are determined from the Poisson distribution to take into account the low statistics in most bins. Total uncertainties are represented with boxes.

$N^{\rm bin}_{i=A}$ at $\sqrt{s} = 2.1250$ GeV for category A in two bins (see more bins in Appendix A).

The signal reconstruction efficiency $\mathcal{E}_i^{\rm MC}(\cos\theta)$ for each category is determined by a dedicated Monte Carlo (MC) simulation for the process $e^+e^- \to n\bar{n}$ at each $\sqrt{s}$ using the MC generator ConExc [32] up to the next-to-leading order, followed by a GEANT4 [33]-based simulation procedure, which mimics the response of various particles in the BESIII detector. A data-driven efficiency calibration $\mathcal{C}_i^{\rm dm}(\cos\theta)$ is achieved for both n and $\bar{n}$ by using the process $J/\psi \to \bar{p}\pi n(p\pi\bar{n})$. A trigger correction $\mathcal{C}_i^{\rm trg}(\cos\theta)$ describing the probability of EMC-based online trigger capturing neutral processes is also applied. In addition, $(1+\delta)_i(\cos\theta)$ is the initial state radiation and vacuum polarization correction. All corrections are multiplied to be $\mathcal{E}_i^{\rm cor}(\cos\theta) = \mathcal{C}_i^{\rm dm}\cdot\mathcal{C}_i^{\rm trg}\cdot(1+\delta)_i$. The details about these corrections are given in Ref. [24].

With the above numbers for the three categories, $|G_M|$ and $R_{\rm em}$ are determined according to Eq. (1) by minimizing the NLL based on the Poisson probability density function. Figure 3 illustrates a simultaneous fitting to data of $\cos\theta_{\bar{n}}$-dependent cross sections at $\sqrt{s} = 2.1250$ and 2.3964 GeV. The fitting results and associated parameters are summarized in Table I. Note that data collected at 12 c.m. energies is grouped into five intervals to maximize the statistical precision of the results. The details on the fitting procedure and values of differential cross sections for the other energy points are listed in Ref. [34].

Various sources of systematic uncertainties are considered for the determination of $|G_E|$, $|G_M|$, and $R_{\rm em}$, including the uncertainties from the luminosity, the category-specific signal event selections, the MC model, the Born cross section input for the signal efficiency determination, the trigger efficiency, and the fit procedure. The uncertainty from the integrated luminosity is determined with large-angle Bhabha scattering to be 1% [28,29]. The uncertainty from the signal event selection is taken into account by using the efficiency corrections for the differences between data and signal MC. By varying $C^{\rm dm}$ within 1σ, the difference on the differential cross section is taken as the systematic uncertainty. The uncertainty in the efficiency determination stemming from the form factor input model to the MC Born cross section is reduced to 1% by iterative efficiency determination and fitting. The uncertainty from the signal event extraction arises from three sources: the signal shape, the background shape, and the fitting range. By changing the signal and background shapes and varying the fitting range, the systematic uncertainty from the signal yield extraction is determined as the largest deviation from the nominal results. The uncertainty from the trigger efficiency is studied with a different parametrization of the detector response, as discussed in Ref. [24]. The overall systematic uncertainties at each bin are summarized in Ref. [34]. The variation of mean values of $R_{\rm em}$ and $|G_M|$ with or without including

TABLE I. The integrated luminosity $\mathcal{L}$, form factor ratios $R_{\rm em} = |G_E|/|G_M|$, electric $|G_E|$, and magnetic $|G_M|$ form factors. The first uncertainties are statistical and the second systematic. The nominal energy for each energy interval is weighted by luminosity and c.m. energy of the corresponding data sample. The lower (upper) energy uncertainty is taken as the difference between the nominal energy and the lowest (highest) energy among the group.

$\sqrt{s}$ (GeV)	$\mathcal{L}$ (pb^{-1})	$R_{\rm em}$	$\lvert G_M\rvert(\times10^{-2})$	$\lvert G_E\rvert(\times10^{-2})$
2.0000	10.1	$0.9\pm0.7\pm0.4$	$18.6\pm5.0\pm3.1$	$17.2\pm8.3\pm4.7$
2.0500	3.34			
2.1250	108	$1.3\pm0.4\pm0.3$	$8.7\pm1.2\pm0.8$	$11.2\pm1.7\pm1.1$
2.1500	2.84			
2.1750	10.6	$1.5\pm0.6\pm0.2$	$6.5\pm1.5\pm0.4$	$9.8\pm1.9\pm0.6$
2.2000	13.7			
2.2324	11.9			
2.3094	21.1			
2.3864	22.5	$0.9\pm0.3\pm0.2$	$8.3\pm0.9\pm0.4$	$7.3\pm2.1\pm1.0$
2.3960	66.9			
2.6454	67.7	$0.6\pm0.9\pm0.7$	$4.4\pm0.8\pm0.3$	$2.5\pm2.9\pm2.9$
2.9500	15.9			

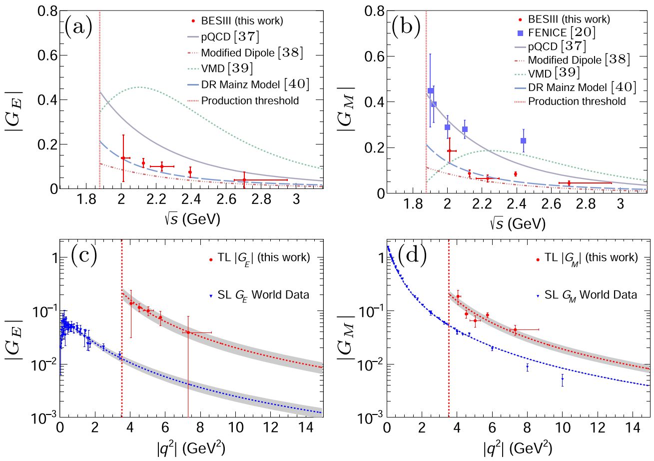

FIG. 4. Results for the separated form factors of the neutron. (a) Electric and (b) Magnetic form factors as a function of $\sqrt{s}$ from this work are shown together with results from the FENICE experiment [20] extracted under the hypothesis $|G_E| = 0$ (blue rectangles) and four different parametrizations [37,40,43]. The vertical red dotted line indicates the production threshold. (c) Electric and (d) Magnetic form factors as a function of $|q^2|$ from this work shown together with results from the world data of SL ones. The fit to TL (SL) data is represented with a red (blue) line and a gray band (95% C.I.). The related fitting results are listed in Table II.

systematic uncertainties during fitting angular distributions is taken as a systematic uncertainty. In total, three categories are used to determine the final results of $R_{\rm em}$ and $|G_M|$ by taking into account correlations of systematic uncertainties at different bins. The uncertainties of $|G_E|$ are propagated from uncertainties of $R_{\rm em}$, $|G_M|$ and their correlations. Table I lists the total systematic uncertainties.

In conclusion, values of $|G_E|$, $|G_M|$, and $R_{\rm em}$ have been extracted at five c.m. energy intervals in the TL region. The results for $R_{\rm em}$ are close to unity considering systematic uncertainties in a wide range of q^2.

Compared with the FENICE results, the values for $|G_M|$ from this work are smaller by a factor of ~2–3 in the range of $\sqrt{s} = 2.0$–2.5 GeV, as shown in Figs. 4(a) and 4(b). The measured $|G_E|$ and $|G_M|$ can be used to test various models to provide a more comprehensive picture of the nucleon structure. Among models such as a parametrization obtained from the pQCD [37], a modified dipole model based on the quark counting rule and analytical extension (MD) [38], a vector meson dominance model (VMD) [39], and a model based on dispersion relations (DR) [40–42], our results show the best agreement with the DR-based model (long-dashed line). Note that the MD parametrization (dot-dashed line) is re-analyzed with the experimental results from this work. The free parameters of the DR-based model are optimized by a fit to the TL $|G_M|$ data, which are extracted for the neutron under the hypothesis that $|G_E| = |G_M|$. The free parameters of the MD model are optimized with a fit to the TL effective FFs. The pQCD

TABLE II. Fitting results with dipole function corresponding to Figs. 4(c) and 4(d).

	$\vert G_E\vert$	
⋯	TL ($q^2 > 4M_n^2$)	SL ($q^2 < 0$)
Formula	$[A/(1-q^2/0.71)^2]$	$[A\tau/(1+B\tau)][1/(1-q^2/0.71)^2]$
Parameters	$A = 3.39 \pm 0.43$	$A = 1.42 \pm 0.08$, $B = 2.17 \pm 0.39$
χ^2/ndf	0.4/4	25/36

	$\vert G_M\vert$	
⋯	TL ($q^2 > 4M_n^2$)	SL ($q^2 < 0$)
Formula	$[A/(1-q^2/0.71)^2]$	$[A/(1-q^2/0.71)^2]$
Parameters	$A = 3.27 \pm 0.28$	$A = 1.899 \pm 0.008$
χ^2/ndf	8.8/4	82/31

based parametrization was initially developed for $|G_E|$ and $|G_M|$, legitimizing the use of these models also for a comparison with $|G_E|$. In contrast, the VMD model predicts different values for $|G_E|$ and $|G_M|$.

The EMFFs derived from data of unpolarized experiments empirically scale like $G_{E,M} \sim (-q^2)^{-2}$ [44] in case of $q^2 \to -\infty$ in the SL region. It is interesting to check whether the TL form factors show any asymptotic behavior. Our results show $|G^n_{E,M}| \sim (q^2)^{-2}$ in the TL region. It is important to test the analyticity of EMFFs as a direct consequence of micro causality and unitarity. As stated in the Phragmèn-Lindelöf (P-L) theorem [45], EMFFs in the TL region can be extended to any direction of the q^2 complex plane. As a result, the numerical values of EMFFs should approach each other for $|q^2| \to \infty$, i.e., $\mathcal{R}^{E,M} \equiv |G^{TL}_{E,M}(q^2)/G^{SL}_{E,M}(-q^2)| \overset{|q^2|\to\infty}{\to} 1$. Figures 4(c) and 4(d) show that the TL $|G_E|$ ($|G_M|$) has no intersections with the SL G_E (G_M), using an extrapolation with current fitting parameters for the neutron. The measured ratios are $\mathcal{R}^E = 5.18 \pm 1.18$ for the electric form factors and $\mathcal{R}^M = 1.72 \pm 0.14$ for the magnetic form factors. The related fitting results are listed in Table II.

In summary, we have separated $|G_E|$ from $|G_M|$ for the neutron within a wide range of q^2 from 4 to 9 GeV^2 with relative uncertainty around 12% for the modulus of the magnetic form factor. This is comparable in accuracy to results from electron scattering in a similar SL region of four-momentum transfer. In the future, further efforts will be made not only at electron accelerators [46,47] but also at electron-positron [48] and proton-antiproton colliders [49] to obtain a global picture of all data in the TL and SL regions which will further deepen our understanding of the nucleon structure.

The BESIII Collaboration thanks the staff of BEPCII and the IHEP computing center for their strong support. This work is supported in part by the National Key R&D Program of China under Contracts No. 2020YFA0406400, No. 2020YFA0406300; National Natural Science Foundation of China (NSFC) under Contracts No. 11635010, No. 11735014, No. 11805124, No. 11835012, No. 11935015, No. 11935016, No. 11935018, No. 11961141012, No. 12022510, No. 12025502, No. 12035009, No. 12035013, No. 12061131003, No. 12122509, No. 12192260, No. 12192261, No. 12192262, No. 12192263, No. 12192264, No. 12192265, No. 12221005; the Chinese Academy of Sciences (CAS) Large-Scale Scientific Facility Program; the CAS Center for Excellence in Particle Physics (CCEPP); Joint Large-Scale Scientific Facility Funds of the NSFC and CAS under Contract No. U1832207; CAS Key Research Program of Frontier Sciences under Contracts No. QYZDJ-SSW-SLH003, No. QYZDJ-SSW-SLH040; 100 Talents Program of CAS; Guangdong Major Project of Basic and Applied Basic Research No. 2020B0301030008; Science and Technology Program of Guangzhou (No. 2019050001); The Double First-Class university project foundation of USTC; The Institute of Nuclear and Particle Physics (INPAC) and Shanghai Key Laboratory for Particle Physics and Cosmology; ERC under Contract No. 758462; European Union's Horizon 2020 research and innovation programme under Marie Sklodowska-Curie grant agreement under Contract No. 894790; German Research Foundation DFG under Contracts Nos. 443159800, 455635585, Collaborative Research Center CRC 1044, FOR5327, GRK 2149; Istituto Nazionale di Fisica Nucleare, Italy; Ministry of Development of Turkey under Contract No. DPT2006K-120470; National Research Foundation of Korea under Contract No. NRF-2022R1A2C1092335; National Science and Technology fund; National Science Research and Innovation Fund (NSRF) via the Program Management Unit for Human Resources and Institutional Development, Research and Innovation under Contract No. B16F640076; Polish National Science Centre under Contract No. 2019/35/O/ST2/02907; Suranaree University of Technology (SUT), Thailand Science Research and Innovation (TSRI), and National Science Research and Innovation Fund (NSRF) under Contract No. 160355; The Royal Society, UK under Contract No. DH160214; The Swedish Research Council; U.S. Department of Energy under Contract No. DE-FG02-05ER41374.

[a]Also at the Moscow Institute of Physics and Technology, Moscow 141700, Russia.

[b]Also at the Novosibirsk State University, Novosibirsk, 630090, Russia.

[c]Also at the NRC "Kurchatov Institute," PNPI, 188300, Gatchina, Russia.

[d]Also at Goethe University Frankfurt, 60323 Frankfurt am Main, Germany.

[e]Also at Key Laboratory for Particle Physics, Astrophysics and Cosmology, Ministry of Education; Shanghai Key Laboratory for Particle Physics and Cosmology; Institute of Nuclear and Particle Physics, Shanghai 200240, People's Republic of China.

[f]Also at Key Laboratory of Nuclear Physics and Ion-beam Application (MOE) and Institute of Modern Physics, Fudan University, Shanghai 200443, People's Republic of China.

[g]Also at State Key Laboratory of Nuclear Physics and Technology, Peking University, Beijing 100871, People's Republic of China.

[h]Also at School of Physics and Electronics, Hunan University, Changsha 410082, China.

[i]Also at Guangdong Provincial Key Laboratory of Nuclear Science, Institute of Quantum Matter, South China Normal University, Guangzhou 510006, China.

[j]Also at Frontiers Science Center for Rare Isotopes, Lanzhou University, Lanzhou 730000, People's Republic of China.

[k]Also at Lanzhou Center for Theoretical Physics, Lanzhou University, Lanzhou 730000, People's Republic of China.

[l]Also at the Department of Mathematical Sciences, IBA, Karachi, Pakistan.

[1] K. G. Wilson, Phys. Rev. D **10**, 2445 (1974).

[2] H. Fritzsch, M. Gell-Mann, and H. Leutwyler, Phys. Lett. **47B**, 365 (1973).

[3] R. Hofstadter and R. W. McAllister, Phys. Rev. **98**, 217 (1955).

[4] R. Hofstadter, Rev. Mod. Phys. **28**, 214 (1956).

[5] V. Punjabi, C. F. Perdrisat, M. K. Jones, E. J. Brash, and C. E. Carlson, Eur. Phys. J. A **51**, 79 (2015).

[6] X. D. Ji, Phys. Rev. Lett. **74**, 1071 (1995).

[7] A. Deur, S. J. Brodsky, and G. F. de Teramond, Rep. Prog. Phys. **82**, 076201 (2019).

[8] H. Atac, M. Constantinou, Z. E. Meziani, M. Paolone, and N. Sparveris, Nat. Commun. **12**, 1759 (2021).

[9] L. N. Hand, D. G. Miller, and R. Wilson, Rev. Mod. Phys. **35**, 335 (1963).

[10] J. Arrington, C. D. Roberts, and J. M. Zanotti, J. Phys. G **34**, 23 (2007).

[11] J. Arrington, K. de Jager, and C. F. Perdrisat, J. Phys. Conf. Ser. **299**, 012002 (2011).

[12] C. F. Perdrisat, V. Punjabi, and M. Vanderhaeghen, Prog. Part. Nucl. Phys. **59**, 694 (2007).

[13] M. R. Yearian and R. Hofstadter, Phys. Rev. **110**, 552 (1958).

[14] S. Pacetti, R. Baldini Ferroli, and E. Tomasi-Gustafsson, Phys. Rep. **550**, 1 (2015).

[15] J. P. Lees *et al.* (*BABAR* Collaboration), Phys. Rev. D **87**, 092005 (2013).

[16] M. Ablikim *et al.* (BESIII Collaboration), Phys. Rev. Lett. **124**, 042001 (2020).

[17] M. Ablikim *et al.* (BESIII Collaboration), Phys. Lett. B **817**, 136328 (2021).

[18] D. Lin, A. Dbeyssi, and F. Maas, Symmetry **14**, 91 (2022).

[19] L. Xia, C. Rosner, Y. D. Wang, X. Zhou, F. E. Maas, R. B. Ferroli, H. Hu, and G. Huang, Symmetry **14**, 231 (2022).

[20] A. Antonelli *et al.* (FENICE Collaboration), Nucl. Phys. **B517**, 3 (1998).

[21] D. Bisello *et al.* (DM2 Collaboration), Z. Phys. C **48**, 23 (1990).

[22] M. N. Achasov, A. Y. Barnyakov, K. I. Beloborodov, A. V. Berdyugin, D. E. Berkaev *et al.* (SND Collaboration), Phys. Rev. D **90**, 112007 (2014).

[23] M. N. Achasov *et al.* (SND Collaboration), Eur. Phys. J. C **82**, 761 (2022).

[24] M. Ablikim *et al.* (BESIII Collaboration), Nat. Phys. **17**, 1200 (2021).

[25] M. Ablikim *et al.* (BESIII Collaboration), Nucl. Instrum. Methods Phys. Res., Sect. A **614**, 345 (2010).

[26] C. H. Yu *et al.*, in *Proceedings of the IPAC2016, Busan, Korea* (JACoW, Geneva, 2016).

[27] Q. H. Yang, L. Y. Dai, D. Guo, J. Haidenbauer, X. W. Kang, and U. G. Meißner, arXiv:2206.01494.

[28] M. Ablikim *et al.* (BESIII Collaboration), Chin. Phys. C **41**, 063001 (2017).

[29] M. Ablikim *et al.* (BESIII Collaboration), Chin. Phys. C **41**, 113001 (2017).

[30] M. Ablikim *et al.* (BESIII Collaboration), Chin. Phys. C **46**, 074001 (2022).

[31] A. Zichichi, S. M. Berman, N. Cabibbo, and R. Gatto, Nuovo Cimento **24**, 170 (1962).

[32] R. G. Ping, Chin. Phys. C **38**, 083001 (2014).

[33] S. Agostinelli *et al.* (GEANT4 Collaboration), Nucl. Instrum. Methods Phys. Res., Sect. A **506**, 250 (2003).

[34] See Supplemental Material at http://link.aps.org/supplemental/10.1103/PhysRevLett.130.151905 for additional descriptions, which includes Refs. [24,35,36].

[35] https://root.cern/download/doc/RooFit_Users_Manual_2.91-33.pdf.

[36] R. Fletcher, Comput. J. **13**, 317 (1970).

[37] D. V. Shirkov and I. L. Solovtsov, Phys. Rev. Lett. **79**, 1209 (1997).

[38] E. Tomasi-Gustafsson and M. P. Rekalo, Phys. Lett. B **504**, 291 (2001).

[39] R. Bijker and F. Iachello, Phys. Rev. C **69**, 068201 (2004).

[40] H. W. Hammer, U. G. Meissner, and D. Drechsel, Phys. Lett. B **385**, 343 (1996).

[41] Y. H. Lin, H. W. Hammer, and U. G. Meißner, Eur. Phys. J. A **57**, 255 (2021).

[42] Y. H. Lin, H. W. Hammer, and Ulf-G. Meißner, Phys. Rev. Lett. **128**, 052002 (2022).

[43] A. Bianconi and E. Tomasi-Gustafsson, Phys. Rev. Lett. **114**, 232301 (2015).

[44] S. J. Brodsky and G. R. Farrar, Phys. Rev. Lett. **31**, 1153 (1973).

[45] E. Titchmarsh, *The Theory of Functions*, 2nd ed, (Oxford University Press, Oxford, 1939).

[46] A. Accardi, J. L. Albacete *et al.*, Eur. Phys. J. A **52**, 268 (2016).

[47] D. P. Anderle *et al.*, Front. Phys. (Beijing) **16**, 64701 (2021).

[48] M. Ablikim *et al.* (BESIII Collaboration), Chin. Phys. C **44**, 040001 (2020).

[49] B. Singh *et al.* (PANDA Collaboration), Eur. Phys. J. A **52**, 325 (2016).

Correction: The omission of the fourth author (S. Ahmed) has been fixed.